*Plasma Medicine* 3(4): 291-314 (2013)

# Nonthermal Plasma-Assisted Trauma Management: Hemostasis of Noncompressible Profuse Hemorrhage

Atharva Amritkar,[a] Becky Cunningham,[b] Bradly Hawkins,[c] Brennan Batalla,[a] David Moore,[b] Eric Thompson,[b] Matt Rossett,[b] Rittick Gupta,[a] Justine Han,[d] & Justin M. Johnson[e,*]

[a]Electrical and Computer Engineering, Rowan University, Glassboro, New Jersey, USA; [b]Mechanical Engineering, Rowan University, Glassboro, New Jersey, USA; [c]Chemical Engineering, Rowan University, Glassboro, New Jersey, USA; [d]Chemical and Biological Engineering, Drexel University, Philadelphia, Pennsylvania, USA; [e]Health Onvector Inc., Camden, New Jersey, USA

[*] **Address all correspondence to Justin M. Johnson:** 200 Federal Street, Suite 300, Camden, NJ 08103; +1 (856) 438-0770; E-mail: jmj@healthonvector.com

**ABSTRACT:** In this manuscript we discuss a chemical kinetic model of blood coagulation by treatment with nonequilibrium atmospheric pressure dielectric barrier discharge. We then add kinetic data into a computational fluid dynamics model of blood flow treated by plasma and show that we are able to induce hemostasis. We then present initial experimental validation of these computational models using *in vitro* bovine blood samples.

**KEY WORDS:** nonthermal plasma; plasma medicine; hemostasis; coagulation; blood; hemorrhage; trauma

## I. INTRODUCTION

Over 40% of combat-related deaths are attributable to uncontrolled bleeding, the majority of those from noncompressible profuse hemorrhage.[1,2] Of the two main current conventional approaches, thermal coagulation creates extensive tissue damage unacceptable for noncompressible combat wounds, while various powder-based coagulants have absorbance capacity that is easily overcome by profuse hemorrhage. Thus, the combat medic requires breakthrough novel tools that effectively stop massive bleeding and that they can employ rapidly and easily. We have recently developed such a breakthrough novel device based on nonthermal nanosecond-pulsed plasma applied directly to a bleeding wound surface.[3–5]

In this paper we simulate, investigate, and optimize the dynamics of flowing and coagulating blood for the case of profuse hemorrhage undergoing direct pulsed plasma treatment, and discuss a prototype system that a combat medic can apply to a real, complex, three-dimensional profusely bleeding wound.

 

## II. BACKGROUND

### A. Nonthermal Plasma-assisted Hemostasis

Recently, a new method has been developed and demonstrated for controlling applied high voltages in nanosecond pulses in order to stabilize a powerful nonequilibrium plasma, making it sufficiently uniform to be directly applied to cells and living tissues without thermal destruction.[6,7] This important innovation is the breakthrough that enables our team to demonstrate effective plasma stimulation of hemostasis, tissue regeneration, and wound healing.[3,8,9]

Effective plasma stimulation of *in vivo* blood coagulation has been demonstrated in experiments with live SKH1 mice. Fifteen seconds of Floating Electrode- Dielectric Barrier Discharge (FE-DBD) plasma treatment is able to coagulate blood at the surface of a cut saphenous vein as well as tail vein of a mouse.[5] In these experiments, only the ability of direct nonthermal plasma treatment to coagulate blood was tested, and the animal was not left alive to test improvement in healing times.

It was demonstrated that direct nonthermal plasma can trigger natural, rather than thermally induced, coagulation processes.[7] It was also observed that the release of calcium ions and change of blood pH level, which could be responsible for coagulation, is insignificant. Instead, the evidence points to selective action of direct nonthermal plasma on blood proteins involved in natural coagulation processes.

Mechanisms of plasma interaction with blood can be deduced from the following facts observed in the experiments with FE-DBD plasma: (1) Plasma can coagulate both normal and anticoagulated blood, but the rate of coagulation depends on the anticoagulant used; (2) plasma is able to alter ionic strength of the solution and change its pH, but normal and anticoagulated blood buffers these changes even after relatively long treatment times; (3) plasma changes the natural concentration of clotting factors significantly, thus promoting coagulation; (4) effects delivered by plasma are nonthermal and are not related to gas temperature or the temperature at the surface of blood; (5) plasma is able to promote platelet activation and formation of fibrin filaments, even in anticoagulated blood. These experimental facts are discussed in further detail below.

(1) Anticoagulants like sodium heparin bind thrombin in the coagulation cascade thus slowing coagulation, while sodium citrate or ethylene diamine tetraacetic acid (EDTA), are designed to bind calcium, an important factor in the cascade, thereby preventing coagulation altogether. Plasma treatment promotes visible coagulation in the presence of all of the above anticoagulants.

(2) Previously, plasma coagulation hypotheses were focused on increases in the concentration of $Ca^{2+}$, which is an important factor in the coagulation cascade. It was suggested that plasma stimulates generation of $Ca^{2+}$ through the redox mecha-

nism provided by hydrogen ions produced in blood in a sequence of ion-molecular processes induced by plasma ions. Validity of the hypothesis was tested experimentally by measuring $Ca^{2+}$ concentration in the plasma-treated anticoagulated whole blood using a calcium-selective microelectrode. Calcium concentration was measured immediately after plasma treatment and remained almost constant for up to 30 s of treatment and then increased slightly for prolonged treatment times of 60 and 120 s. Although plasma is capable of coagulating anticoagulated blood within 15 s, no significant change occurs in calcium ion concentration during the typical time of blood coagulation in discharge treated blood. *In vivo*, the pH of blood is maintained in a very narrow range of 7.35–7.45 by various physiological processes. The change in pH by plasma treatment (about 0.1 after 30 s) is less than the natural variation of pH, which indicates that the coagulation is probably not due to the pH change in blood.

(3) FE-DBD treatment of whole blood samples was shown to change concentrations of various proteins participating in the coagulation cascade. Plasma treatment is shown to "consume" coagulation factors (proteins and enzymes) and a visible film is formed on the surface of the treated samples. The plasma treatment effect was diminished by either increasing the sample volume or keeping the surface area fixed, indicating that plasma treatment initiates clot formation at the surface, not throughout the volume. A corresponding kinetic model of the plasma-assisted blood coagulation indicates a twofold decrease in clot formation time with plasma treatment.[5]

(4) When the surface of blood is protected by a thin aluminum foil, which prevents contact between blood and FE-DBD plasma but transfers all the heat generated by plasma, no influence on blood is observed. This suggests a nonthermal mechanism of the plasma-stimulated blood coagulation.

(5) The final step in the natural biological process of blood coagulation is the production of thrombin which converts fibrinogen into fibrin monomers that polymerize to form fibrin microfilaments. FE-DBD plasma treatment of fibrinogen solution in physiological medium coagulates it, which is confirmed visually through a change in the color of the solution (from clear to milky-white) and through dynamic light scattering.[10] Of note is that plasma does not influence fibrinogen through a pH or temperature change. FE-DBD treatment, however, is unable to polymerize albumin (directly not participating in coagulation cascade) as no change in its behavior is observed both visually and through dynamic light scattering (DLS). Thus nonthermal plasma selectively affects proteins (specifically, fibrinogen) participating in the natural coagulation mechanism. Morphological examination of the clot layer by scanning electron microscopy (SEM) further proves that plasma does not "cook" blood, but initiates and enhances natural sequences of blood coagulation processes. Activation followed by aggregation of platelets is the initial step in the coagulation cascade and conversion of fibrinogen into fibrin is the final step in the coagulation cascade. It was shown that the extensive platelet activation, platelet aggregation, and fibrin formation follows after the FE-DBD plasma treatment.[3,10]

## III. MATERIALS AND METHODS

### A. Computational Fluid Dynamics (CFD) Model

To create a suitable computational model of the biochemical phenomenon of blood coagulation, various modeling approaches, geometries, and methods were evaluated. COMSOL 4.3 Multiphysics solver was used together with a 3D flow-through pipe model. Changes in blood viscosity induced by plasma treatment were modeled through the introduction of a point source of heat into the flow and the liquid was given a temperature-dependent viscosity.

### B. Kinetic Coagulation Model

MATLAB was used to solve the governing reactions in blood coagulation with respect to time. These reactions were taken from a blood coagulation model that was previously developed by Fridman et al.[5] This mathematical model determines the rate of reaction of the different factors used to create thrombin among other factors that assist in the coagulation of blood. In this kinetic model the effect of plasma is introduced through rate increase of reactions related to calcium ion release from blood cells as was previously reported.[3,5] A second model is currently being developed to include the reactions associated with platelet activation.

### C. Measurements of Calcium Ion Concentration in *In Vitro* Blood Samples

Four samples of bovine blood (Lampire Biological Laboratories, Pipersville, PA) were tested to obtain baseline concentration of calcium ions. Each sample was prepared using a chromogenic reagent and a calcium assay buffer kit (BioVision Incorporated, Milpitas, CA). The reagent included *o*-cresolphthalein which, when reacted with calcium ions, forms a chromogenic complex identifiable at 575 nm. All samples were prepared in 75 μL microcuvettes.

A standard curve was created using a calcium standard diluted with distilled water to give samples of 0, 1.2, 2, and 4 μg $Ca^{2+}$/mL. Blood samples were measured using a UV-Vis Spectrophotometer (Hitachi U-2900 Double Beam Spectrophotometer). Preparation involved mixing 50 μL of sample, 90 μL chromogenic reagent, and 60 μL calcium assay buffer in a cuvette. The reaction was incubated for 10 min and then measured at 575 nm. Absorbance measurements obtained were correlated with the concentration of $Ca^{2+}$ using the standard curve. See Table 1.

### D. Measurement of Power Dissipated in the Discharge

The DBD device, constructed based on the schematics introduced by Fridman et al.,[5]

**TABLE 1:** Results of calcium ion measurements

| Sample | Absorbance | μg $Ca^{2+}$/mL |
|---|---|---|
| 7 mM | 0.212 | 24.55 |
| 4 mM | 0.167 | 19.31 |
| Control | 0.156 | 18.03 |

was connected to a transformer to easily manipulate the electrode power output. The electrode wire was placed through an ammeter and connected through a voltage probe to power resistors with a total impedance of 300 kΩ. This impedance was selected as an approximation of the impedance from the electrode treatment of dry (no additional moisture) skin.[11] The measurements from the ammeter and the voltage probe where both used to calculate the power dissipated in the discharge.

## E. Countering the Effect of Anticoagulant in Blood

The *in vitro* blood samples used in this experimental study were anticoagulated by EDTA (ethylenediaminetetraacetic acid). EDTA binds calcium ions and thus prevents coagulation cascade activation. Satchidanandam et al. report that addition of 4 mM $Ca^{2+}$ countered the effect of EDTA and allowed blood to coagulate normally.[12] As such, the concentration of calcium chloride needed to counteract the EDTA anticoagulant added to the blood for preservation was calculated as part of this study. Twelve vials were filled with 4 mL of bovine blood. A 70 mM solution of anticoagulant neutralizer (ACN) was prepared using high-purity calcium chloride. This base solution was titrated with saline in order to dilute further test solutions to produce desired concentrations. All of the blood samples were heated at 37°C for 30 min before testing. Once at the appropriate temperature, 100 μL of the ACN solutions were added to the blood vials. The vials were then placed in an upright stand and observed every minute until coagulation: Once the entire volume of the test tube solidified the blood was deemed coagulated.

## F. Blood Viscosity Measurement

As blood is coagulating, its viscosity changes drastically and thus we opted to use the viscosity change as an indicator of coagulation (viscosity was measured by Hemathix Blood Analyzer SCV-200, Health Onvector Inc., Camden, NJ). Vials were each filled with 4 mL of bovine blood and constituted with 100 μL of ACN solution to counteract the anticoagulant effects. Subsequently, each blood sample was poured into a dish and exposed to plasma (see schematic in Fig. 1 and photograph of the treatment procedure in Fig. 2). After exposure, the sample viscosity was measured using the Hemathix automated scanning capillary viscometer.

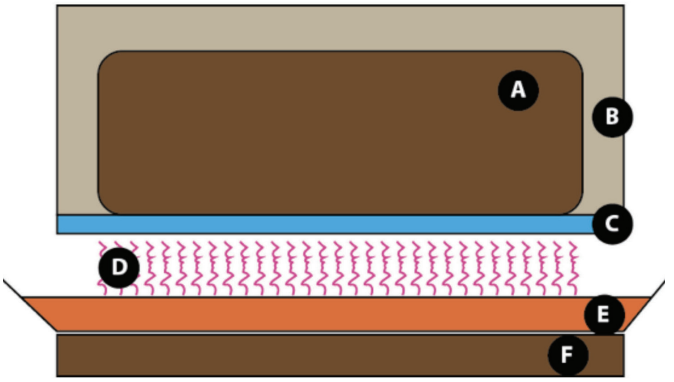


**FIG. 1:** Schematic of the blood treatment setup: (A) copper core of the high-voltage electrode; (B) plastic housing for the electrode; (C) quartz dielectric; (D) plasma generated between quartz surface and blood surface; (E) blood sample; and (F) grounded plate

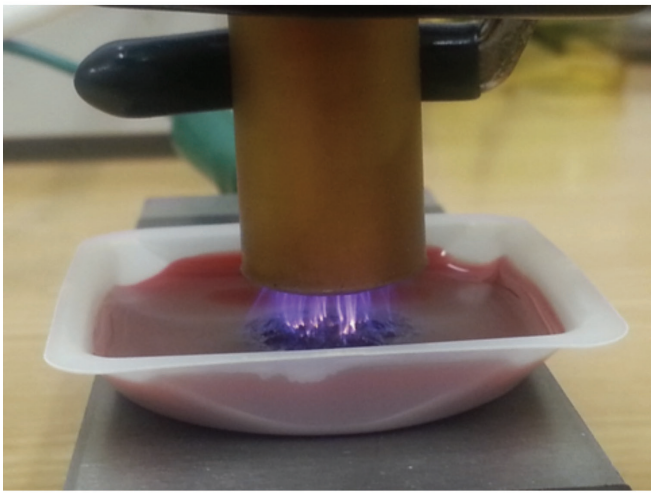

**FIG. 2:** Photograph of blood being treated by plasma

## G. Plasma Treatment of Flowing Blood

To validate plasma treatment of flowing blood we have constructed a setup simulating a bleeding arteriole of ~1.5 mm diameter. To accomplish this we have placed 100 mL of blood with ACN solution 30 cm above the laboratory benchtop surface and allowed it to flow through a channel cut in an aluminum plate (Figs. 3 and 4). In this setup, approximate pressure at the "bleeding cut" is 25 mmHg which is comparable to the cut

arteriole blood pressure. The channel was covered with a dielectric film with a ~1.5 mm hole punched in it to simulate a cut.

## IV. RESULTS AND DISCUSSION

### A. Computational Fluid Dynamics Model of Plasma-assisted Coagulation of Flowing Blood

Simple pipe flow simulations were successfully carried out. The challenging portion of creating this model was finding a physical mechanism that replicated blood coagula-

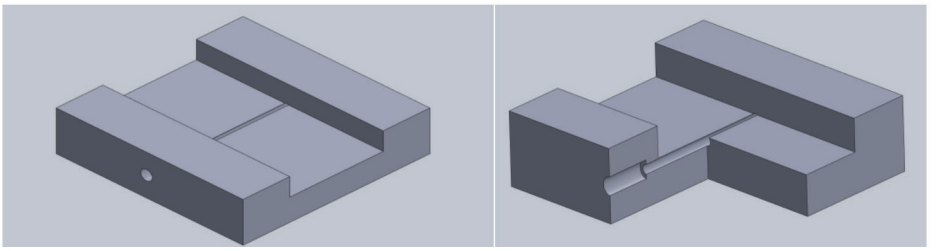

**FIG. 3:** Drawing of the bleed plate (BP) used to imitate active bleeding on tissue surface. A Teflon film is placed over the bleed channel. Afterwards, a small hole is punched just above the bleed channel to allow for blood flow representing an open cut

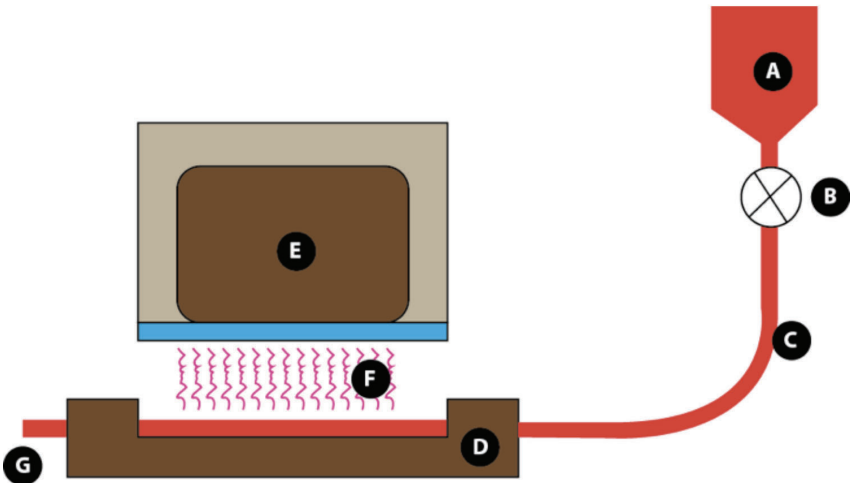


**FIG. 4:** Schematic of the flowing blood setup: (A) a reservoir containing blood, elevated 30 cm from the setup to allow for 25 mmHg pressure at the treatment zone; (B) blood flow control valve; (C) blood-compatible tubing; (D) bleed plate, described previously; (E) plasma treatment electrode; (F) area of blood treatment; and (G) post-treatment blood flowing out of the system

tion in COMSOL 4.3 using the available modules. The initial mechanism attempted to change blood viscosity over time. This was done using a point heat source applied to the surface of the pipe and changing the physical properties of the working fluid to increase viscosity with temperature. The "heat transfer in fluids" physics module was employed to apply the point heat source. The rate at which temperature changed viscosity was given by an exponential function called "viscRate" as seen in Eq. (1).

$$\text{viscRate} = 0.035*\exp(k*T) \quad \textbf{Eq. 1}$$

The 0.035 is the original blood viscosity in centipoise, $k$ is a selected constant, and $T$ is the temperature of the fluid. This model, shown in Fig. 5, continuously failed to converge when solving its mesh if the selected $k$ constant of the viscRate equation defined above was given significant weight.

Following the initial experience the model was modified. The focus was redirected to finding a working coagulation mechanism. The new geometry was changed to a 2D pipe 2 cm in diameter and 8 cm long. This model would represent a large group of vessels and a wider system of blood flow. Once again water was the working fluid and non-Newtonian physics was ignored. Free and porous flow physics was employed. A cross section in the center of the pipe was designated as the porous matrix. A second outlet was added to the model as the same position as the porous matrix. This outlet simulated the presence of a cut on the surface of the flow system. The cut outlet is 1 cm

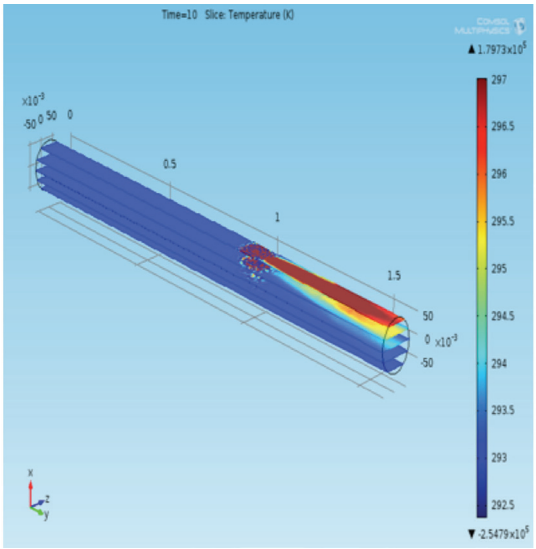


**FIG. 5:** Temperature distribution in viscosity mechanism model. Here the temperature distribution from the point heat source is clearly visible. Once the $k$ value in Eq. (1) reached a threshold that would allow fluid viscosity to increase with temperature, the program failed to converge on a solution

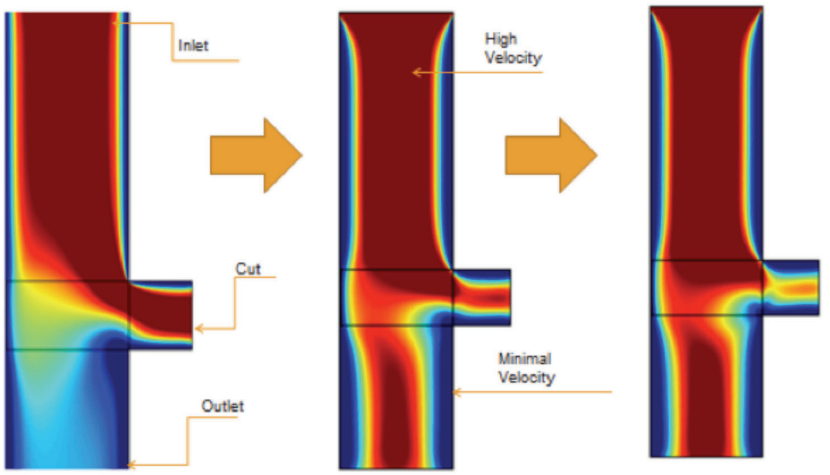


**FIG. 6:** Porosity coagulation mechanism for flow system. At the end of the study time period, fluid flow has been reduced through the wound outlet on the side of the main channel

wide, representing a wound of moderate severity. Using the same initial conditions as the previous model, the goal of this model was not to change the fluid properties but to change the characteristics of the porous matrix over time. Using heat transfer, the porous matrix would decrease in porosity over time, eventually stopping flow to the cut outlet. Visible in Fig. 6, the simulation run based on these parameters represented the process of coagulation mathematically as reductions in porosity, with the wound closing over time starting from the point heat source placed on the edge of the cut.

The coagulation mechanism was expanded to include plasma treatment considerations. In normal coagulation, generation of the chemical species used in the process usually starts at one point near the edge of a cut by tissue factor. This was represented by the point heat source in the model. During plasma treatment, there is an increase in generation of the species that start the biological process of coagulation. The species are created as several points on the wound surface area as opposed to a singular location at the edge of the remaining tissue factor. In order to simulate this, additional point heat sources were added to the model while all other factors from the previous model were controlled and maintained at the same values. The result shown in Fig. 7 was a much more thorough coagulation of the cut domain within the study time range.

It is important to note that at this stage of modeling blood coagulation, focus was put on development of a coagulation mechanism that could possibly simulate the process. As a result, optimization of geometry, flow physics, and boundaries were secondary to the construction of a well-working coagulation model. Ten watts were selected as a working estimation of power for the point heat source. The relationship of temperature to porosity was maintained as a linear function of $1/T$. The material chosen for the porous matrix was brick. The Cp was increased to 4000 J/kg·K and the thermal conduc-

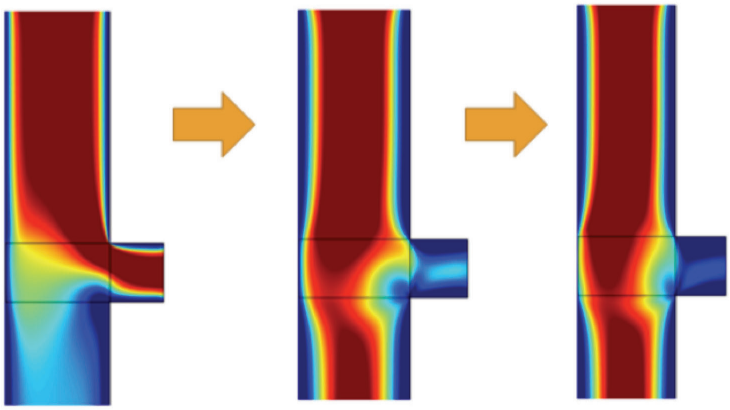

**FIG. 7:** Porosity mechanism with added heat sources. It is evident here that fluid velocity through the wound outlet has been reduced to a negligible amount and most of the fluid has been redirected into the main channel of flow

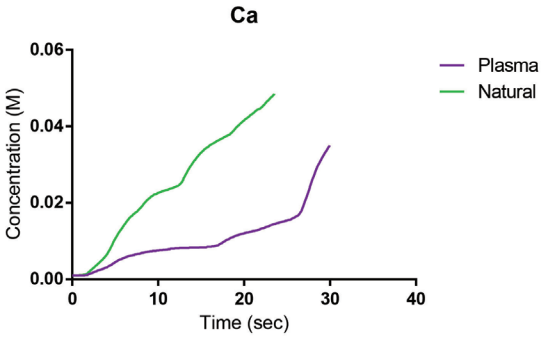


**FIG. 8:** Calcium ion concentration

tivity was reduced to 0.005 W/m·K in order to slow down the heat transfer within the selected time domain of 15 min.

## B. Kinetic Coagulation Model

Presented here are illustrative case data resulting from kinetic modeling of plasma influence on concentrations of various blood constituents and key blood coagulation proteins and their complexes, taking place in blood as it coagulates (Figs. 8–37).

As can be observed, the tendency is for plasma treatment to increase the concentration of the activated blood coagulation factors (in most cases, large proteins with catalytic activity) and increase the concentration of critical coagulation proteins. In general,

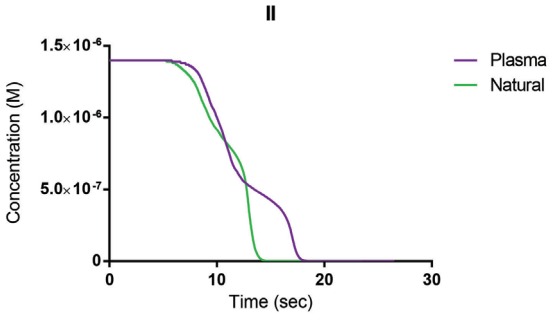


**FIG. 9:** Factor II concentration

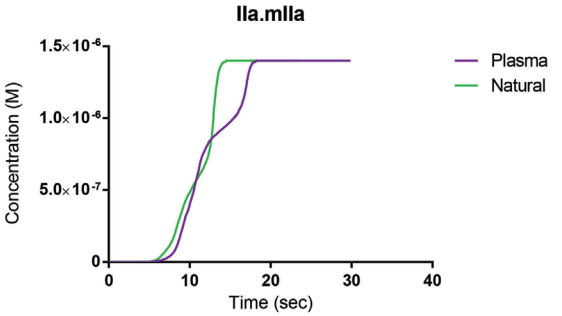


**FIG. 10:** Concentration of complex formed with active Factor II and Factor MIIa

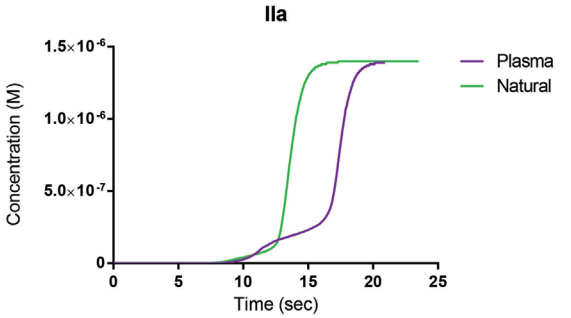


**FIG. 11:** Concentration of active Factor II

from the kinetic modeling we see most of the plasma influence to take place around the 10-s mark, while natural coagulation is activated later. The only conclusion that can be made from this simplified coagulation model thus far is that plasma has some influence on the coagulation cascade and this phenomenon needs to be studied in further detail. In

**TABLE 2:** Results from $CaCl_2$ concentration test

| Concentration of $CaCl_2$ | Coagulation time |
|---|---|
| 0 mM (control) | Did not coagulate |
| 0.1 mM | Did not coagulate |
| 1 mM | Did not coagulate |
| 4 mM | 7±1 min |
| 7 mM | 6±2 min |
| 70 mM | Did not coagulate |

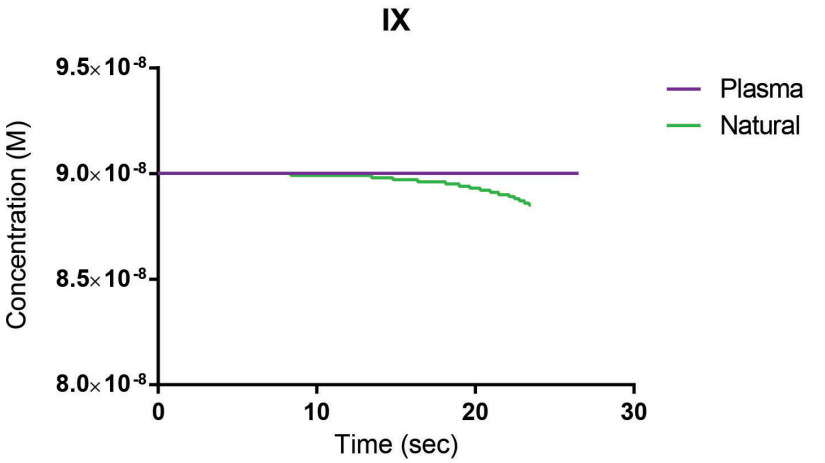


**FIG. 12:** Concentration of Factor IX

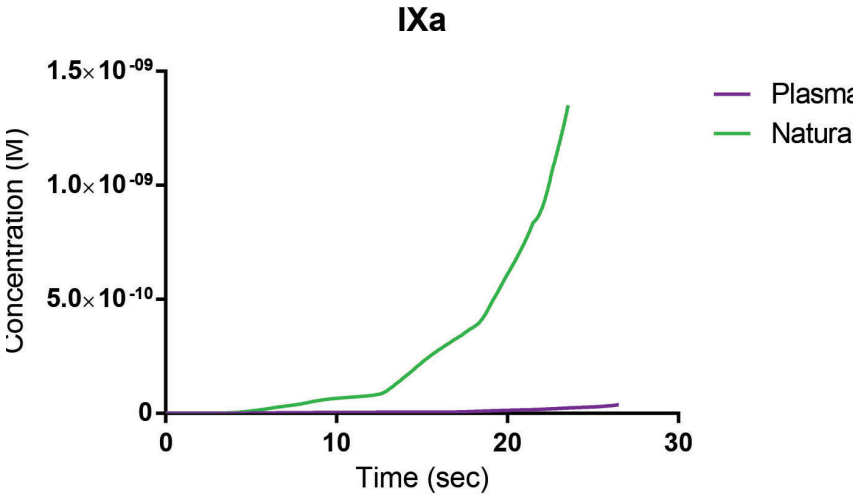


**FIG. 13:** Concentration of active Factor IX

the future we plan to include also the extrinsic pathway, involving platelets.

## IV. *IN VITRO* BLOOD COAGULATION STUDY

### A. Calcium Chloride Concentration Experiment

The results from the calcium chloride concentration experiment can be seen in Table 2.

The 7 mM solution coagulated blood more quickly than the 4 mM solution. However, less moisture was left in the 4 mM solution over the same observed time period, evidencing a more complete coagulation reaction. After noting the results and observations of the experiment it was decided that the 4 mM ACN solution was the optimal choice for the following experimentation blood preparation.

### B. Measured Viscosity with Plasma Treatment

A graph showing the systolic (high-shear) and diastolic (low-shear) viscosities in millipoise units of each blood sample from the first plasma treatment experiment can be seen in Fig. 38. Systolic blood viscosity was reported using measurements of blood at a high shear rate of 300 $s^{-1}$, and diastolic blood viscosity was measured and reported at a low

**TABLE 3:** Viscosity results from the second plasma treatment experiment

| Test | Systolic viscosity | Diastolic viscosity |
|---|---|---|
| Control 1 | 31.4 | 77.5 |
| Control 2 | 30.4 | 76.8 |
| Maximum power: 10 s plasma treatment | 31.5 | 75.5 |
| Maximum power: 20 s plasma treatment | Blood coagulated in capillary viscometer | |
| Maximum power: 30 s plasma treatment | Blood coagulated in capillary viscometer | |

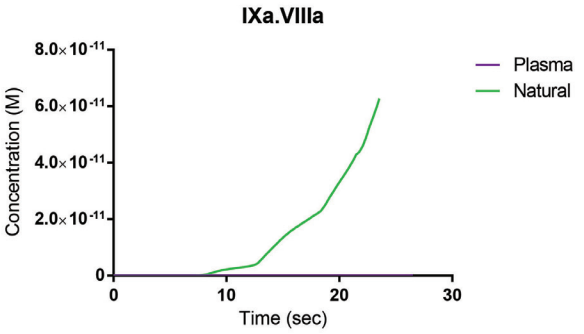


**FIG. 14:** Concentration of complex formed with active Factor IX and active Factor VIII

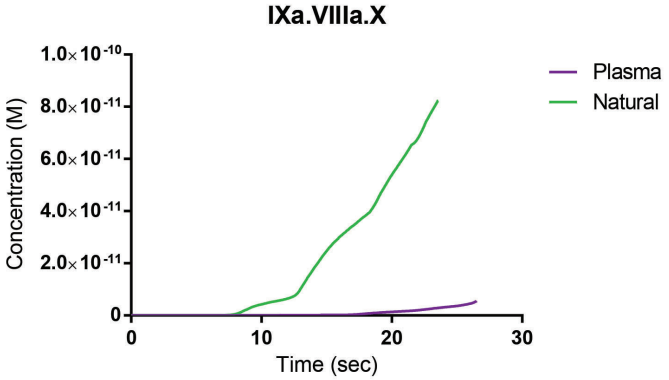


**FIG. 15:** Concentration of complex formed between active Factor IX, active Factor VIII, and Factor X

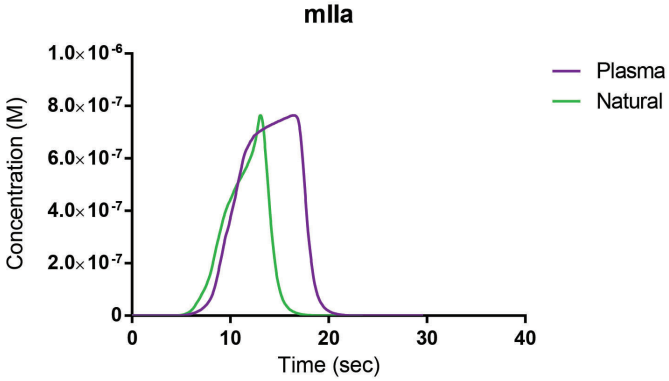


**FIG. 16:** Concentration of Factor MIIa

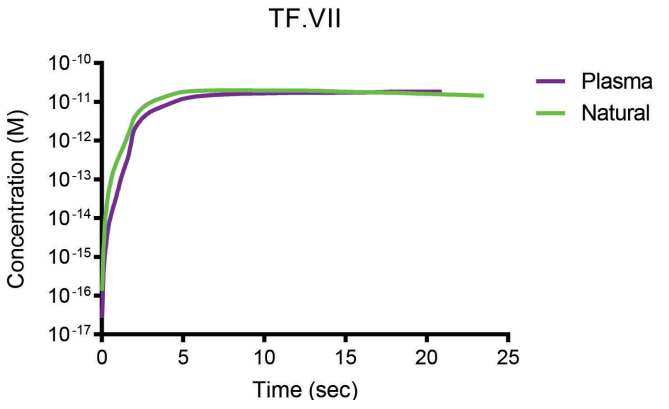


**FIG. 17:** Concentration of complex formed between Tissue Factor and Factor VII

shear rate of 5 $s^{-1}$.

As can be seen from Fig. 38 blood viscosity decreased with plasma treatment as evidenced by the drop in diastolic viscosity with increased plasma exposure. This may have been due to the formation of thrombi and heterogeneous regions of hyperviscosity. These thrombi and partially-coagulated portions of blood samples could not be scanned in the capillary viscometer used in this study and therefore had to be separated from the remaining blood, shown in Fig. 39. This left the remaining less viscous blood to be tested.

Because the coagulated masses and visible thrombi increased with plasma treatment, their physical removal from treated blood samples caused blood viscosity measurements to be lower rather than higher with plasma treatment. This experiment was run a second time. The results are noted in Table 3.

The trend of decreasing viscosity appeared to continue in this experiment. However, the blood samples for the last two plasma treatments coagulated too quickly for reasonable conclusions to be confirmed. Future studies will employ both capillary viscometers like the Hemathix and rotational viscometers such as the Brookfield to investigate the coagulation effect of plasma on viscosity further.

## C. Timed Coagulation with Plasma Treatment

In order to obtain clearer and more consistent results the team altered the procedure as discussed in the Methods and Materials section of this paper. The results are displayed in Table 4.

It can be seen that plasma exposure does reduce coagulation time. The maximum exposure was limited to 30 s due to material limits of the electrode that was employed to produce the dielectric barrier discharge.

A noteworthy phenomenon that became clear in this experiment was the appearance of structures in the blood samples after plasma treatment, shown in Fig. 38. While further research towards understanding the consistent appearance of these structures is needed, the origin of the branches may be speculated: they are the coagulated blood surface imprints of the actual plasma discharge streamers when they make contact with

**TABLE 4:** Coagulation times of stationary blood samples in an open-air environment

| Plasma treatment time | Coagulation time (min) |
|---|---|
| No plasma treatment | 56 |
| 10 s plasma treatment | 49 |
| 20 s plasma treatment | 43 |
| 30 s plasma treatment | 45 |

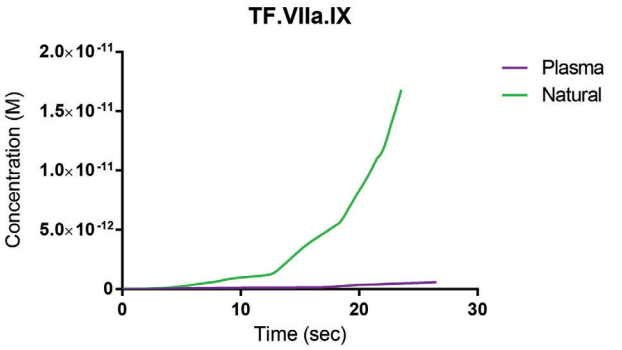


**FIG. 18:** Concentration of complex formed between Tissue Factor, active Factor VII, and Factor IX

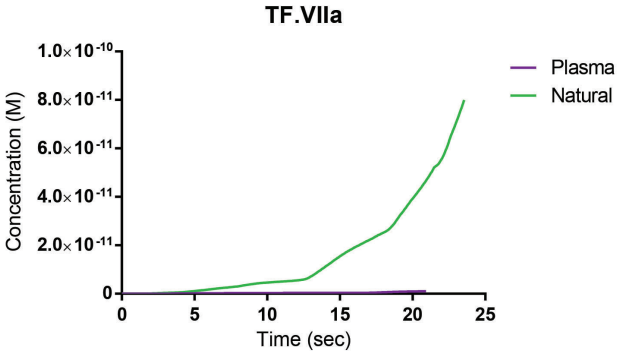


**FIG. 19:** Concentration of complex formed between Tissue Factor and active Factor VII

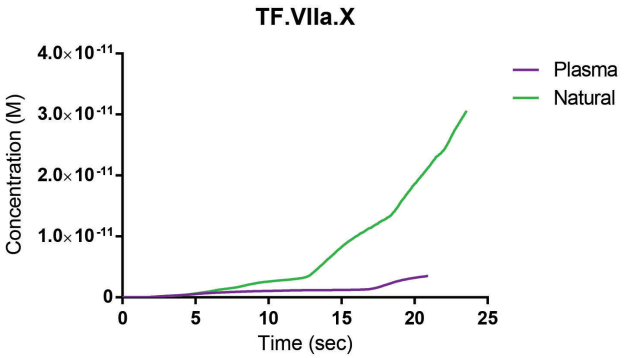


**FIG. 20:** Concentration of complex formed between Tissue Factor, active Factor VII, and Factor X

the blood surface. At those points the blood coagulated instantly (Fig. 40).

## E. Plasma Treatment with Flowing Blood

Figure 41 shows the plasma treatment of flowing blood. Due to the complications of

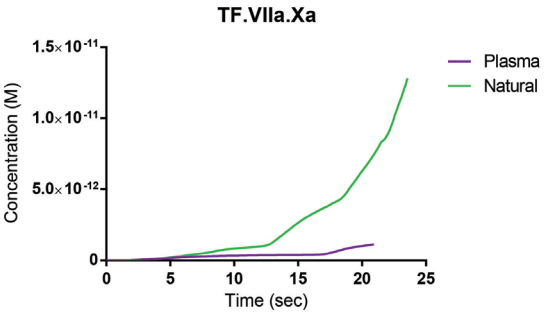


**FIG. 21:** Concentration of complex formed between Tissue Factor, active Factor VII, and active Factor X

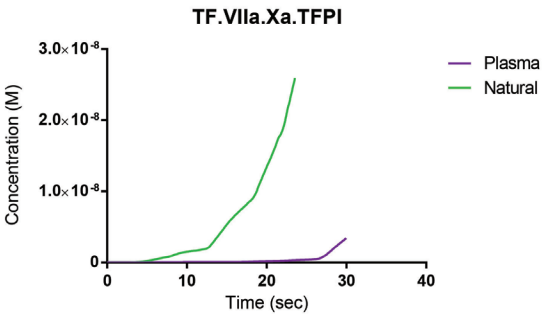


**FIG. 22:** Concentration of complex formed between Tissue Factor, active Factor VII, active Factor X, and Tissue Factor Pathway Inhibitor

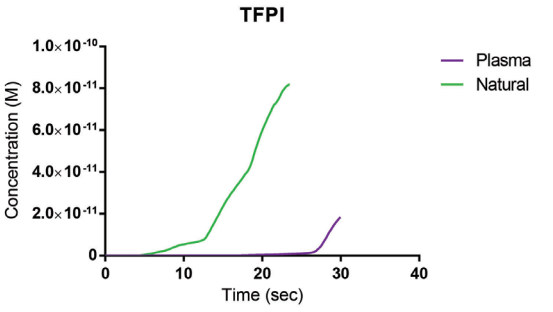


**FIG. 23:** Concentration of Tissue Factor Pathway Inhibitor

the experimental design, blood flow was blocked through the channel in the presence of plasma treatment and new incoming blood simply "burst" through the formed blood

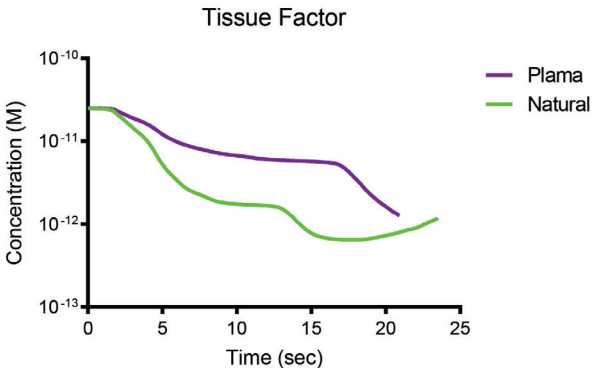


**FIG. 24:** Concentration of Tissue Factor

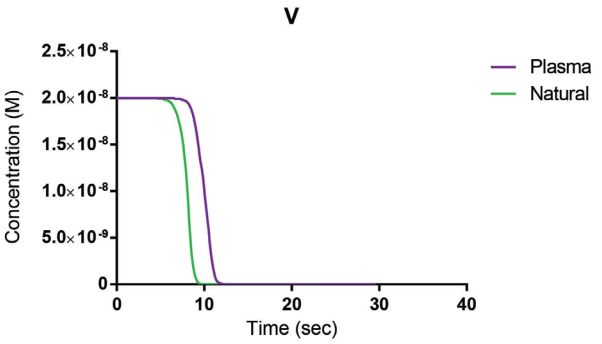


**FIG. 25:** Concentration of Factor V

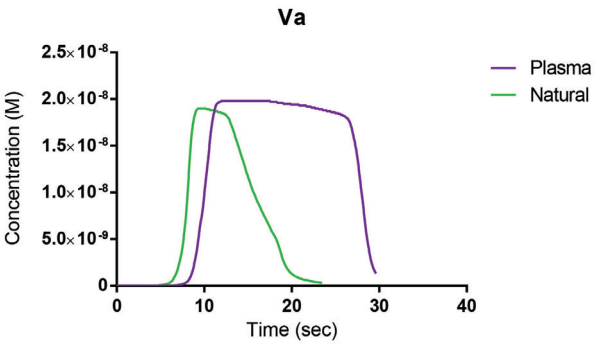


**FIG. 26:** Concentration of active Factor V

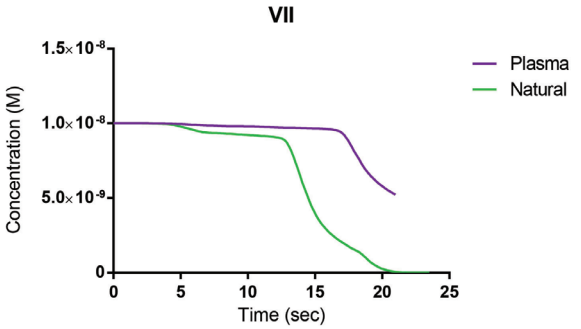


**FIG. 27:** Concentration of Factor VII

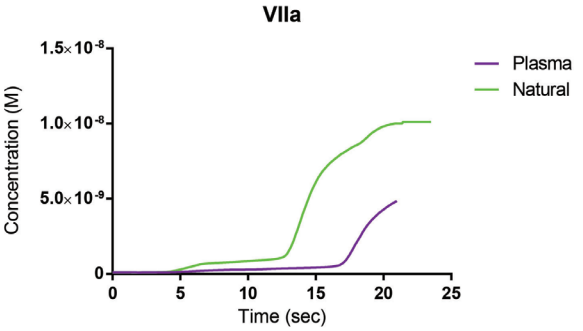


**FIG. 28:** Concentration of active Factor VII

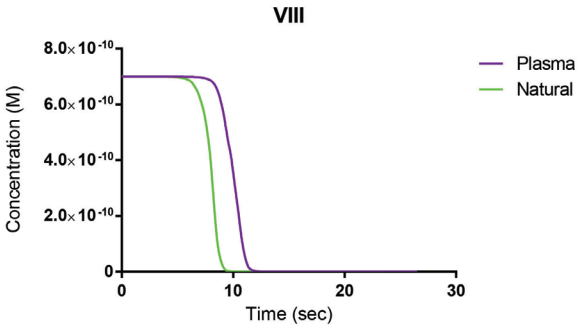


**FIG. 29:** Concentration of Factor VIII

clot. While this may be a positive indication of plasma treatment effectiveness in stopping flowing blood, further research and more effective experimental design are needed to optimize this system.

## VI. CONCLUSIONS

In this article we showed nonequilibrium plasma coagulation of flowing blood. Specif-

ically, we discussed the kinetics of blood coagulation when plasma species are interacting with blood coagulation cascade proteins and the dynamics of blood coagulation when a cut is treated with plasma. Finally, we show that out kinetic and dynamic models

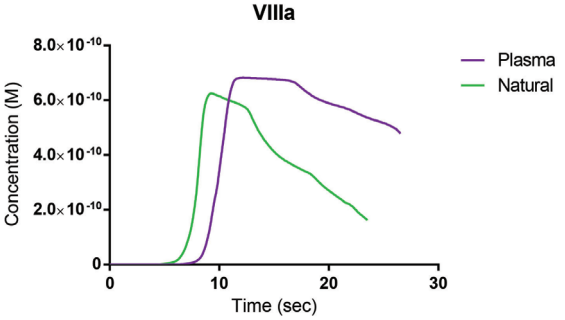


**FIG. 30:** Concentration of active Factor VIII

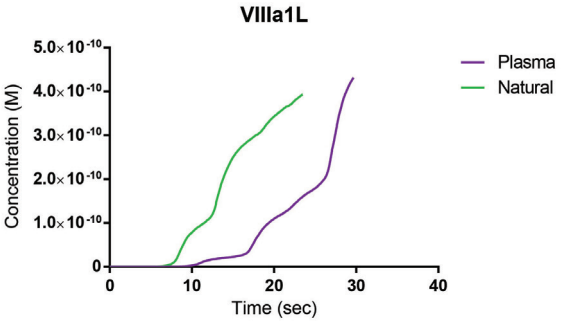


**FIG. 31:** Concentration of Factor VIIIa1L

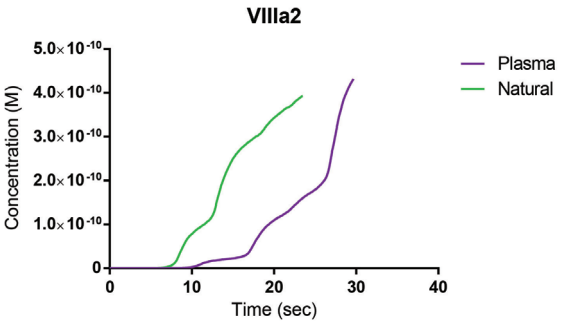


**FIG. 32:** Concentration of Factor VIIIa2

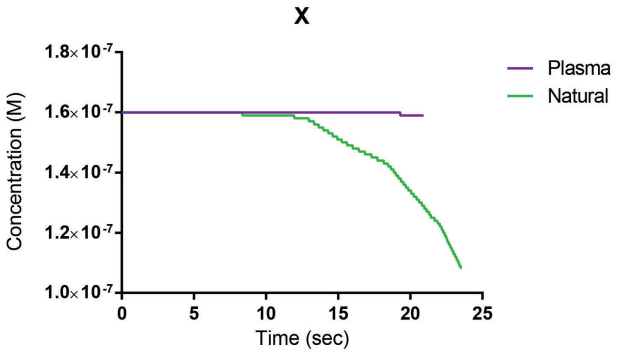


**FIG. 33:** Concentration of Factor X

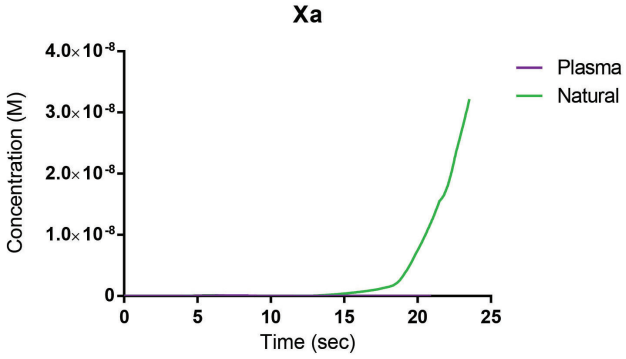


**FIG. 34:** Concentration of active Factor

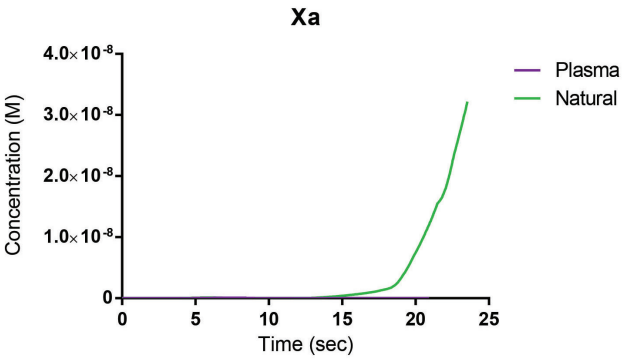


**FIG. 35:** Concentration of complex formed between active Factor X and Tissue Factor Pathway Inhibitor

can be experimentally validated in a stationary and in a flowing blood setup. Many unanswered questions remain and further testing is needed to validate some of the initial experiments presented in this paper. Additional research studies are planned to investi-

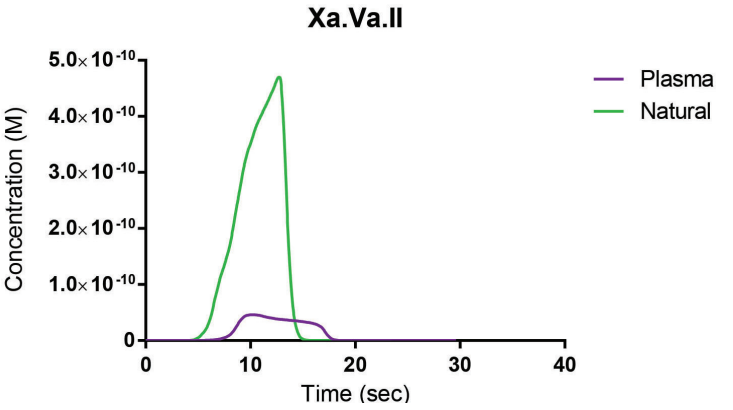


**FIG. 36:** Concentration of complex formed between active Factor X, active Factor V, and Factor II

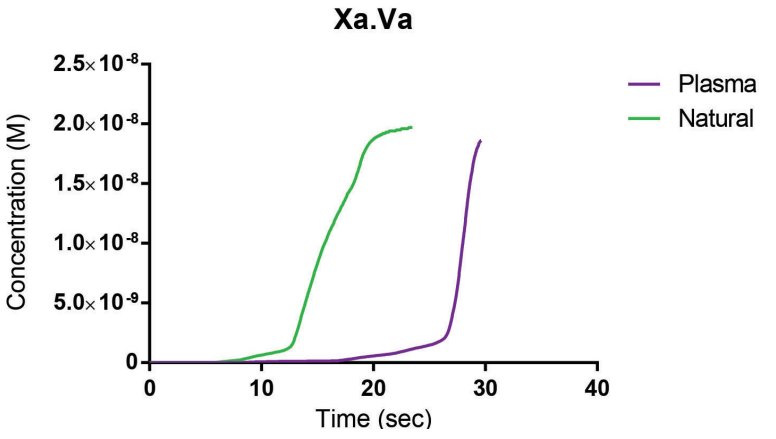


**FIG. 37:** Concentration of complex formed between active Factor X and active Factor V

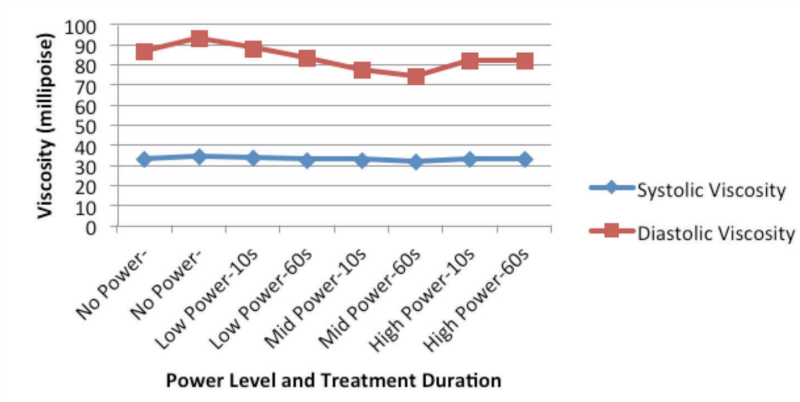


**FIG. 38:** The general trend visible occurs within the diastolic viscosity. There is a drop in viscosity measured by the Hemathix and total exposure to plasma increases.

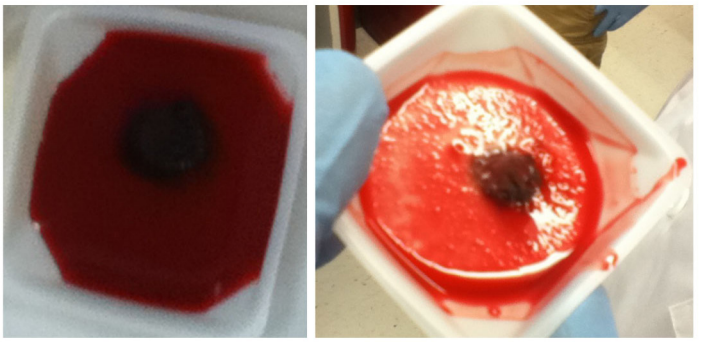

**FIG. 39:** Coagulated mass created during a high-power treatment is left behind prior to viscosity measurement

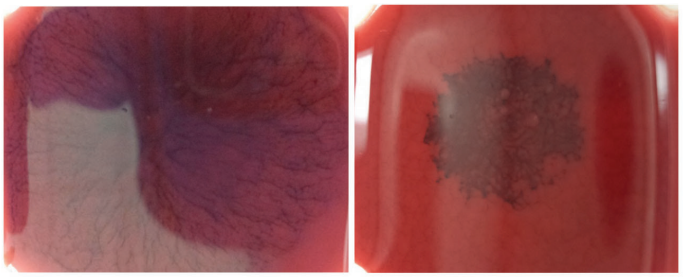

**FIG. 40:** Veinlike structures appearing in blood samples after plasma treatment. There is a noted correlation between treatment time and location and the position and intensity of the vein structures.

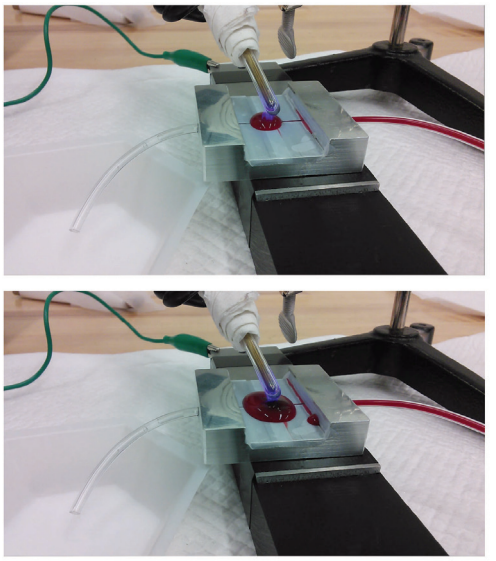

**FIG. 41:** The DBD is placed directly on top of the "cut" channel on the bleed plate. A noticeably darker area of blood is visible in the second image (bottom). Due to the large flow rate of the blood coming from the cut, it was difficult to determine what the effect of plasma on active bleeding was. Future tests will be conducted with slower flow rates.

gate the mechanisms of plasma-assisted coagulation of flowing blood.

## REFERENCES


1. Burnett LR, Richter JG, Rahmany MB, Soler R, Steen JA, Orlando G, Abouswareb T, Van Dyke ME. Novel keratin (KeraStat™) and polyurethane (Nanosan®-Sorb) biomaterials are hemostatic in a porcine lethal extremity hemorrhage model. J Biomater Appl. 2014;28(6):869–79.
2. Lashof-Sullivan M, Shoffstall A, Lavik E. Intravenous hemostats: challenges in translation to patients. Nanoscale. 2013;5(22):10719–28.
3. Fridman G, Friedman G, Gutsol A, Shekhter AB, Vasilets VN, Fridman A. Appl Plasma Med Plasma Process Polym. 2008;5(6):503–33.
4. Fridman G, Shereshevsky A, Jost M, Brooks A, Fridman A, Gutsol A, Vasilets V, Friedman G. Floating electrode dielectric barrier discharge plasma in air promoting apoptotic behavior in melanoma skin cancer cell lines. Plasma Chem Plasma Process. 2007;27(2):163–76.
5. Fridman G, Peddinghaus M, Ayan H, Fridman A, Balasubramanian M, Gutsol A, Brooks A, Friedman G. Blood coagulation and living tissue sterilization by floating-electrode dielectric barrier discharge in air. Plasma Chem Plasma Process. 2006;26(4):425–42.
6. Dobrynin D, Wu A, Kalghatgi S, Park S, Shainsky N, Wasko K, Dumani E, Ownbey R, Joshi S, Sensenig R, Live pig skin tissue and wound toxicity of cold plasma treatment. Plasma Med J. 2011;1(1):93–108.
7. Dobrynin D, FridmanG, Friedman G, Fridman A, Physical and biological mechanisms of direct plasma interaction with living tissue. New J Phys. 2009;11:115020.
8. Chakravarthy K, Dobrynin D, Fridman G, Friedman G, Murthy S, Fridman AA. Cold spark discharge plasma treatment of inflammatory bowel disease in an animal model of ulcerative colitis. Plasma Med. 2011;1(1):3–19.
9. Wu AS, Kalghatgi S, Dobrynin D, Sensenig R, Cerchar E, Podolsky E, Dulaimi E, Paff M, Wasko K, Arjunan KP. Porcine intact and wounded skin responses to atmospheric nonthermal plasma. J Surg Res. 2013 Jan;179(1):e1–e12.
10. Kalghatgi SU, FridmanG, Cooper M, Nagaraj G, Peddinghaus M, Balasubramanian M, Vasilets VN, GutsolA, Fridman A, Friedman G. Mechanism of blood coagulation by nonthermal atmospheric pressure dielectric barrier discharge plasma. IEEE Trans Plasma Sci. 2007;35(5, Part 2):1559–66.
11. Rosell J, Colominas J, Riu P, Pallas-Areny R, Webster JG. Skin impedance from 1 Hz to 1 MHz. IEE Trans Biomed Eng. 1988;35(8):649–51.
12. Kumar P, Satchidanandam V. Ethyleneglycol-bis-(β-aminoethylether) tetraacetate as a blood anticoagulant: preservation of antigen-presenting cell function and antigen-specific proliferative response of peripheral blood mononuclear cells from stored blood. Clin Diagnost Lab Immunol. 2000;7(4):578–83.